

APPLYING LAGRANGIAN FLUID MECHANICS TO INFER SCALAR SOURCE DISTRIBUTIONS FROM CONCENTRATION PROFILES IN PLANT CANOPIES

M.R. RAUPACH

CSIRO Centre for Environmental Mechanics, GPO Box 821, Canberra, A.C.T. 2601 (Australia)

(Received October 17, 1988; revision accepted February 28, 1989)

ABSTRACT

Raupach, M.R., 1989. Applying Lagrangian fluid mechanics to infer scalar source distributions from concentration profiles in plant canopies. *Agric. For. Meteorol.*, 47: 85–108.

It is well known that gradient-diffusion theory does not describe the transfer of scalar entities (such as heat, water vapour, CO₂ and pollutant gases) through the air in and just above plant canopies. An effective replacement is offered by an analytic Lagrangian method for calculating the concentration field of a scalar emanating from a steady spatially extensive source in an inhomogeneous flow. The method can be labelled “localized near-field” or LNF theory. This paper first summarizes the assumptions and results of the LNF theory, leading to a simple solution for the “forward problem” of predicting the mean scalar concentration profile $C(z)$ maintained by a given source density profile $S(z)$. It is then shown how the theory can be applied to solve the “inverse problem” of inferring $S(z)$ from measurements of $C(z)$.

INTRODUCTION

Efforts to describe and understand canopy–atmosphere exchange are driven largely by two motives: (1) to model attributes of the canopy microclimate, such as the flux and concentration profiles for heat and water vapour, using simple canopy and atmospheric parameters as inputs; and (2) to use knowledge of the exchange process to infer biological or physical properties of the canopy which are otherwise hard or impossible to measure: in particular, to deduce flux and source–sink profiles for CO₂ and trace contaminants from measurements of the associated concentration profiles. This paper specifically addresses the second goal, but the techniques outlined here are also applicable to the first.

To set the scene, we consider an arbitrary scalar entity such as heat, water vapour, CO₂ or a contaminant gas, letting $S(z)$ be its source density profile (with a sink being a negative S), $F(z)$ its vertical scalar flux density and $C(z)$ its mean concentration profile, where z is height above ground. For steady

conditions in an extensive, uniform canopy, advection is negligible and the scalar conservation equation reduces to

$$S(z) = dF/dz, \quad F(z) = F_g + \int_0^z S(z) dz \quad (1)$$

where F_g is the scalar flux density from the ground at $z=0$. The next requirement is a relationship between $C(z)$ and $F(z)$, or $C(z)$ and $S(z)$; in other words, a description of turbulent transfer in the canopy. The most common assumption has been the gradient-diffusion relationship

$$F(z) = -K(z) dC/dz \quad (2)$$

where $K(z)$ is an eddy diffusivity, a property of the turbulence in the canopy. It is now common knowledge that eq. 2 is inadequate in plant canopies, because $K(z)$ is hopelessly erratic and cannot be specified uniquely in terms of turbulence properties. Most dramatically, Denmead and Bradley (1985, 1987) observed regions of countergradient flux, where K is negative, for heat, water vapour and CO_2 transfer within a pine forest. The reason for the failure of eq. 2 in canopies is that vertical scalar transfer is maintained by eddies with length scales of the order of the canopy height, h , so the vertical mixing process is not "fine grained" with respect to the $C(z)$ profile. This contradicts the most basic assumption in the gradient-diffusion approach (Corrsin, 1974).

The search for a physically sound description of turbulent transfer in canopies follows two broad lines of enquiry: Eulerian (fixed frame) and Lagrangian (fluid following). The Lagrangian approach, which is pursued here, aims to predict the mean scalar concentration field from a given source density by tracking an ensemble of "marked fluid particles" carrying the scalar (Monin and Yaglom, 1971; Durbin, 1983). Since the wind field must be specified, Lagrangian dispersion theory is concerned only with scalar dispersion; this is the main limitation of the Lagrangian relative to the Eulerian approach, which can predict simultaneously the wind and scalar fields. The principal compensating advantage of the Lagrangian approach is that a fluid-following framework allows the effects of fluid particle history to be properly taken into account. Because turbulent motions are coherent over finite length and time scales, fluid particle velocities exhibit persistence over time intervals of order T_L , the Lagrangian integral time scale; consequently, the dispersion of a scalar cloud is non-diffusive in the near field, where the cloud travel time is small relative to T_L , and diffusive in the far field where the travel time is large.

In a plant canopy, these are important considerations because the dominant turbulent eddies are of the scale of the canopy height and hence persist in their motion through much of the canopy. The scalar field therefore reflects a superposition of both near-field and far-field dispersive influences, because the scalar material at any observing point emanates from both nearby and distant

source points. The consequences were examined by Raupach (1987) using a simple analysis of dispersion in homogeneous turbulence, which showed that persistence alone accounts for the main qualitative features of scalar transfer in a canopy: the observed shapes of concentration profiles, the appearance of countergradient fluxes in some circumstances and the important part played by turbulent transport in the vertical scalar flux budget. That so much can be predicted from such simple assumptions suggests that the Lagrangian approach has promise in the canopy context.

Lagrangian dispersion theory, in its usual form, deals with the “forward problem” of predicting the concentration field, C , from a given, externally specified source density, S . However, most applications of a scalar transfer theory for plant canopies also involve the “inverse problem”: predicting S from a given concentration profile, C . Solving the inverse problem is clearly the whole key to the second of the two practical goals mentioned at the outset, that of inferring sources and sinks from concentration data. The first goal, microclimate modelling, also carries an implicit inverse component, since for most scalars of interest (heat, water vapour and pollutants in particular) the source or sink density, S , depends on the scalar concentration, C , so one must find both S and C together. In short, most applications of a canopy transfer theory depend either explicitly or implicitly on a solution to the inverse problem.

The main purpose of this paper is to develop a practical approach to the inverse (S from C) problem, and to illustrate its application to source–sink inference from concentration data. Naturally, a solution of the inverse problem relies upon prior adequate understanding of the forward problem. To achieve this, we use the “localized near-field theory” (LNF theory for short) developed by Raupach (1989) to predict the concentration profile, C , produced by a source profile, S , in a canopy. The paper is organised as follows: a thumbnail sketch of the turbulent wind field in a canopy is given, summarizing experimental knowledge of the wind statistics needed for Lagrangian predictions of vertical scalar transfer. The LNF theory is summarized for predicting C from S , drawing from Raupach (1989) and a discretized, linear relationship between the source and concentration profiles, S and C is developed; this offers a solution to the inverse problem. Finally, the practicalities of applying the solution of the inverse problem to real concentration data are explored.

THE CANOPY WIND FIELD AND SOME OF ITS IMPLICATIONS

Lagrangian predictions of vertical dispersion require information about the probability density function of the vertical Lagrangian velocity $W(t)$ of a marked fluid particle. In practice, sufficient information is obtained from the standard deviation σ_w and skewness Sk_w of w , the Eulerian (fixed-point) vertical velocity. Information is also needed about the persistence of $W(t)$, which may be characterized by the Lagrangian integral time scale T_L . This is defined

as the integral over the time delay (from zero to large delay) of the autocorrelation function for $W(t)$; more intuitively, T_L is the time scale over which $W(t)$ remains correlated with itself due to the persistence of the turbulent motion. Unfortunately, T_L is an intrinsically Lagrangian quantity which is difficult to infer from Eulerian velocity measurements. However, some guidance is available from the scale relationship of Corrsin (1963) for isotropic turbulence

$$T_L = \beta L_w / \sigma_w \quad (3)$$

where β is a constant of order 1 and L_w is the Eulerian length scale for w , usually found from single-point data by using Taylor's frozen-turbulence hypothesis $L_w = UT_E$, U being the mean streamwise wind speed and T_E the single-point Eulerian time scale for w . Tennekes and Lumley (1972) argued from assumed spectral shapes that $\beta = 4/3$, while Snyder and Lumley (1971) measured $\beta = 1$ in grid turbulence. It must be stressed that eq. 3 can only ever give a rough estimate of T_L in a canopy because of the strong anisotropy of the turbulence and because of high turbulence intensities which lead to the failure of Taylor's hypothesis. However, circumstantial evidence (mentioned near the end of the paper) suggests that eq. 3 with $\beta = 1$ provides a reasonable estimate of T_L in a canopy.

Figure 1 shows a collection of direct measurements of σ_w , L_w/σ_w and Sk_w for seven different canopies (two corn canopies, two forests and three wind tunnel models) with the canopy height, h , and the friction velocity, u_* , as normalizing length and velocity scales. These data are drawn from the review of Raupach (1988); see Table 1 for details about the canopies and measurements. In almost all cases, the thermal stability was neutral or nearly so. All the data are from single vertical profiles, positioned to avoid obvious interference from nearby canopy elements. More detailed measurements in two of the canopies (WT Strips and Moga, see Table 1) indicated that this intuitively sensible position-

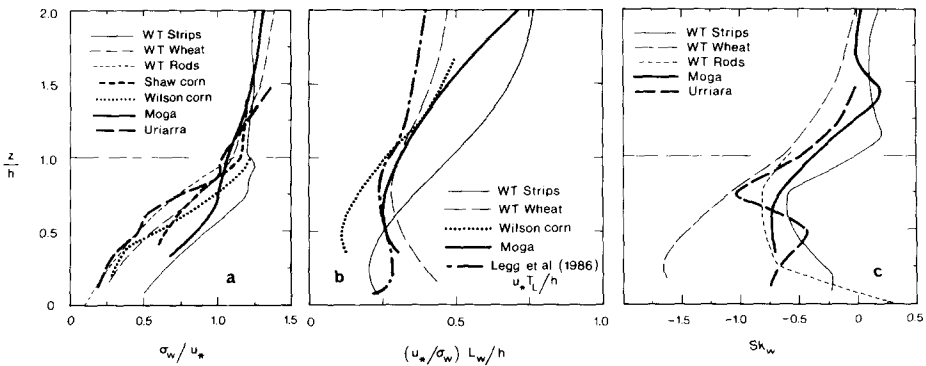


Fig. 1. Profiles of (a) σ_w , (b) L_w/σ_w and (c) Sk_w in seven canopies listed in Table 1. Normalizing scales are the canopy height h and the friction velocity u_* .

TABLE 1

Properties of seven canopies in Fig. 1^a

Canopy	Reference	h	LAI	$\bar{u}(h)/u_*$	Sensors ^b
WT Strips	Raupach et al. (1986)	60 mm	0.23	3.3	T/T
WT Wheat	^c	47 mm	0.50	4.1	T/T
WT Rods	Seginer et al. (1976)	19 cm	1.0	5.0	X/X
Shaw Corn	Shaw et al. (1974)	260 cm	3.0	3.6	C/F
Wilson Corn	Wilson et al. (1982)	225 cm	2.9	3.2	C,F/F
Moga Forest	^c	12 m	1.0	2.9	C,S3/S3
Uriarra Forest	Denmead and Bradley (1987)	16,20 m	4.0	2.5	C/S1

^aWT denotes wind tunnel; LAI leaf area index. ^bSensors (mean/turbulence): C = cup anemometer; F = split-film servo-driven anemometer; X = X-configuration hot-wire anemometer; T = co-planar triple hot-wire anemometer; S1 = single-dimension (vertical) sonic anemometer; S3 = three-dimensional sonic anemometer. ^cPapers in preparation by Y. Brunet, J.J. Finnigan and M.R. Raupach.

ing strategy provided a reasonable estimate of a truly horizontally averaged profile.

A common structure is evident, even though the canopies vary widely in type, height, area index and foliage distribution. Above the canopy, σ_w varies little (Fig. 1(a)), though there is a tendency for σ_w/u_* to increase with height z , from a value of ~ 1.1 at $z=h$ to a typical surface-layer value of ~ 1.25 at $z \geq 2h$. Within the canopy, the turbulence is quite inhomogeneous, with σ_w decreasing rapidly as z decreases. The rate of decrease varies between canopies, being slowest for the WT Strips canopy (colloquially known as the “tombstone canopy”, because of the resemblance of the element array to a graveyard), where strong streamwise vortices form in the wake at the top of each bluff element. In all canopies, the probability density of w is non-Gaussian: the skewness Sk_w is negative and usually between -0.5 and -1 within the canopy. This is consistent with the known dominance of turbulence in the canopy by gusts –energetic, downward incursions of air into the canopy space from the faster moving flow above (Finnigan and Raupach, 1987). The dominant turbulent eddies are also quite coherent and persistent, with streamwise and vertical length scales, L_u and L_w , of order h and $h/3$, respectively, at $z=h$ (Raupach, 1988). Such coherence implies that T_L is of the same order as the canopy time scale h/u_* . If the constant β in eq. 3 is taken as 1, then the data in Fig. 1(b) suggest that $T_L \approx 0.3h/u_*$ in the canopy, with little height variation. This result is in fair agreement with an independent determination of T_L by Legg et al. (1986), inferred from measurements of far-field diffusivity in the plume from a lateral line heat source at height $0.8h$ in the WT Strips canopy; their T_L profile is also shown in Fig. 1(b).

In summary, canopy turbulence is (a) inhomogeneous, (b) persistent and (c) non-Gaussian (where the lettering corresponds to properties shown by the

frames in Fig. 1). The techniques for handling each of these characteristics in a Lagrangian framework are different and lead to a kind of hierarchy of Lagrangian theories for tackling the forward (C from S) problem. The turbulence characteristics are best approached in the order (b), (a), (c). At the most basic level, (c), persistence alone is a fundamental and essential characteristic of turbulence, which can be studied for homogeneous, Gaussian turbulence using the classical analytic approach of Taylor (1921) and Batchelor (1949). This Lagrangian analysis quickly yields elegant and far-reaching results which were applied by Raupach (1987) to illustrate the importance of persistence in plant canopies, as already mentioned. However, the simple analytic approach is restricted in its pure form to dispersion in steady, homogeneous turbulence. At the opposite extreme in complexity is the numerical or "random-flight" approach, which aims for a general description of dispersion in turbulence incorporating all three of the characteristics (b), (a) and (c). Unfortunately, random-flight models can suffer from fundamental mathematical problems in non-Gaussian turbulence (Sawford, 1986; Thomson, 1987) and, furthermore, the calculations are both lengthy and stochastically noisy. These difficulties represent formidable barriers to the application of the random-flight approach for microclimate modelling and source-sink inference in canopies.

To obtain a theory which is both practical and reasonably realistic, Raupach (1989) developed an analytic Lagrangian theory for dispersion from continuous, spatially extensive sources in turbulence with persistence (b) and inhomogeneity (a), but without non-Gaussian properties (c). This theory occupies a middle level in the hierarchy of complexity, lying between the analytic homogeneous-turbulence and the numerical random-flight theories. For reasons mentioned later, an appropriate label is LNF theory. The theory is based on two approximations which are exact in the homogeneous-turbulence limit, but remain adequate in the inhomogeneous turbulence typically found in canopies. The result is an expression for the concentration profile, $C(z)$, from a given source density profile, $S(z)$, which effectively replaces eq. 1 and, of course, admits the possibility of countergradient transfer in appropriate circumstances. The question of whether it is justifiable to neglect the non-Gaussian aspects of canopy turbulence can be answered by comparing the LNF theory with a random-flight theory (with due regard to the problems mentioned in the last paragraph). It turns out, as will be indicated below, that this assumption is reasonable in most cases. The next two sections outline the LNF theory for the forward (C from S) problem.

BASIC RESULTS FROM LAGRANGIAN DISPERSION THEORY

This section summarizes some necessary basic material. Provided that the Reynolds number is high enough, the dispersal of a scalar released from a source in a turbulent flow is statistically equivalent to the dispersal of an ensemble of marked fluid particles. To find the ensemble-averaged properties of the scalar

cloud (or the time-averaged properties of the cloud, in the case of a steady source in a steady flow), it suffices to assume that the marked particles all move independently. We consider dispersal in only one dimension, the vertical, writing $Z(t)$ for the height and $W(t) = dZ/dt$ for the vertical Lagrangian (fluid-particle-following) velocity of a marked particle. If unit mass of the scalar is released from an instantaneous point source at $z = z_0$ and $t = t_0$, the ensemble-averaged concentration field $C(z, t)$ is equal to the particle transition probability $P(z, t; z_0, t_0)$. This is the conditional probability density that $Z(t) = z$, given that $Z(t_0) = z_0$; i.e., $P dz$ is the probability that a particle with a trajectory passing through the source at time t_0 will pass at a later time, t , through a height element dz , located at z . The superposition principle then yields the mean concentration for a general, extensive source with density $S(z, t)$

$$C(z, t) = \iint P(z, t; z_0, t_0) S(z_0, t_0) dz_0 dt_0 \quad (4)$$

We restrict our attention temporarily to steady, homogeneous turbulence with no mean vertical velocity, and consider the vertical dispersal of the scalar from an instantaneous point release of unit mass (say from $z_0 = 0$, $t_0 = 0$). For this case, the evolution of the ensemble-mean scalar cloud depth $\sigma_Z(t) = \langle Z(t)^2 \rangle^{1/2}$ (where angle brackets denote an ensemble average) is given by the kinematic equation of Taylor (1921)

$$\frac{d\sigma_Z^2}{dt} = 2\sigma_w^2 \int_0^t r_L(s) ds \quad (5)$$

where $r_L(s) = \langle W(t)W(t+s) \rangle / \sigma_w^2$ is the autocorrelation function of W at time lag s . A good approximation for $r_L(s)$ is $\exp(-s/T_L)$, where T_L is the Lagrangian integral time scale for vertical velocity. Equation 5 then gives

$$\sigma_Z^2(t) = 2\sigma_w^2 T_L^2 [t/T_L - 1 + \exp(-t/T_L)] \quad (6)$$

Since both $W(t)$ and $Z(t)$ have distributions which are approximately Gaussian in homogeneous turbulence (Batchelor, 1949), it follows that P , and hence C , are given by

$$C(z, t) = P(z, t; 0, 0) = \frac{1}{(2\pi)^{1/2} \sigma_Z(t)} \exp\left[-\frac{z^2}{2\sigma_Z^2(t)}\right] \quad (7)$$

Although the cloud shape is always Gaussian, eq. 6 shows that the cloud depth behaves differently in the limits of small and large t/T_L , known as the near-field and the far-field limits, respectively

$$\sigma_Z(t) \rightarrow \sigma_w t \quad (t/T_L \rightarrow 0, \text{ near field}) \quad (8a)$$

$$\sigma_Z(t) \rightarrow [2\sigma_w^2 T_L (t - T_L)]^{1/2} \quad (t/T_L \rightarrow \infty, \text{ far field}) \quad (8b)$$

In the near field, persistence causes $W(t)$ to differ little from $W(0)$ and the

particle trajectories $Z(t)$ to depart little from straight lines, so the cloud depth grows linearly with t . In the far field, on the other hand, the effects of persistence are negligible and $Z(t)$ behaves as a random walk, just as for a diffusion process. Hence, the dispersion is diffusive in the far field, but non-diffusive in the near field.

Equations 6–8 specify the actual behaviour of the cloud. In the LNF theory, it is also necessary to consider a hypothetical “diffusion cloud” which spreads diffusively at all times, both far field and near field, and matches the real cloud as closely as possible in the far field. The diffusion cloud has a “diffusion transition probability”, P_f , which satisfies the diffusion equation

$$\frac{\partial P_f}{\partial t} = \frac{\partial}{\partial z} \left[K_f \frac{\partial P_f}{\partial z} \right] \quad (9)$$

where K_f is the diffusivity of the medium. To match the real and diffusion clouds in the far field, it is necessary that $P \rightarrow P_f$ as $t/T_L \rightarrow \infty$. This can be satisfied by noting that for a diffusion cloud released at position $z=0$ and time $t=t_0$ in homogeneous, steady conditions (so that K_f is constant), the solution of eq. 9 is a Gaussian P_f , like eq. 7, with depth $\sigma_{zf}(t) = [2K_f(t-t_0)]^{1/2}$. Comparison with eq. 8b shows that the best match between the real and diffusion clouds in the far field occurs when

$$K_f = \sigma_w^2 T_L \quad (10a)$$

$$t_0 = T_L \quad (10b)$$

Equation 10a defines the far-field eddy diffusivity, which characterizes both the diffusion cloud and the real cloud in its far-field (diffusive) state. It is clear that the real and diffusion clouds can never match in the near field, where persistence causes the real cloud to grow linearly with travel time, whereas the diffusion cloud always grows with the square root of travel time. The result is that the real cloud spreads slower than the diffusion cloud in the near field (since $t^{1/2}$ grows much faster than t when t is small). It follows that the best far-field match is achieved when the diffusion cloud is “handicapped” by being released after the real cloud; eq. 10b shows that the optimum handicap is a time interval T_L . Figure 2 illustrates the spread of the two clouds.

In inhomogeneous turbulence, σ_w and T_L may both depend on z (and on t as well, if the turbulence is unsteady). In these circumstances, there is no analogue of the analytic homogeneous-turbulence result for P , eqs. 6 and 7. However, provided that the inhomogeneity is not too strong, there is still an approximate match in the far field ($t/T_L \rightarrow \infty$) between P and a diffusion transition probability P_f which satisfies eq. 9 with the inhomogeneous far-field diffusivity $K_f(z) = \sigma_w^2(z) T_L(z)$. The approximation of P by P_f in the far field becomes progressively worse as the inhomogeneity increases; available evidence (Sawford, 1984) indicates that the approximation is satisfactory in the

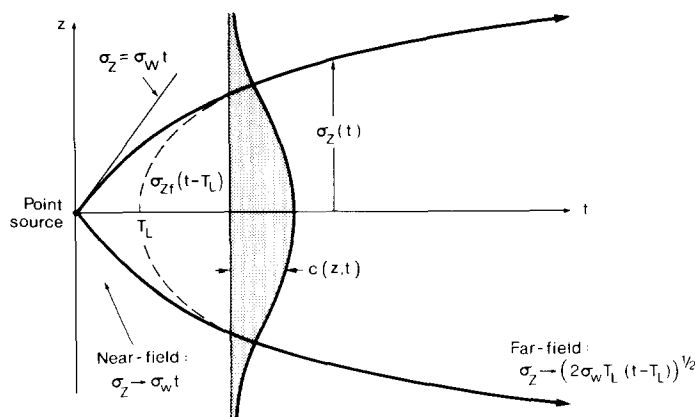


Fig. 2. Real and diffusion clouds dispersing in the z dimension from an instantaneous point source in homogeneous turbulence.

near-neutral atmospheric surface layer and in plant canopy turbulence, but unsatisfactory in a free convection surface layer.

LOCALIZED NEAR-FIELD (LNF) THEORY FOR SCALAR TRANSFER IN A CANOPY

We now consider scalar dispersal from a spatially extensive source in a plant canopy, where the turbulence is vertically inhomogeneous and is specified by given profiles $\sigma_w(z)$ and $T_L(z)$. The problem is: given the concentration $C(z_R)$ at a reference level z_R above (but close to) the canopy, what concentration profile $C(z)$ is produced below z_R by a horizontally uniform source in the canopy, with source density profile $S(z)$? For simplicity, attention is restricted here to the non-advective case of steady conditions and large uniform horizontal fetch x [though the theory is not restricted to this case, the extension to advective conditions being given by Raupach (1989)]. It is necessary to appreciate the nature of the non-advective limit by noting that as x increases, the transfer becomes entirely vertical and the scalar conservation equation tends towards the simple balance $S = dF/dz$. Furthermore, the difference $C(z) - C(z_R)$ becomes independent of x , even though C itself continues to increase with x (see Raupach, 1987, Fig. 1). Therefore, in the non-advective limit, $C(z) - C(z_R)$ is the same as for time-dependent dispersion in one dimension from a steady source with density $S(z)$, turned on at $t=0$ and producing a concentration profile $C(z, t)$. This observation transforms the problem into that of finding the steady, large-time limit of $C(z, t) - C(z_R, t)$.

The essence of the LNF method is to find P for inhomogeneous turbulence, and hence $C(z, t)$ from eq. 4, by making two assumptions. Both become exact only as the inhomogeneity vanishes, but the resulting theory is an adequate approximation for inhomogeneities at least as great as those found in typical

plant canopies. Assumption I is that P may be approximated by P_f in the far field, or more precisely: for large travel times $t - t_0$, the transition probability $P(z, t; z_0, t_0)$ for each source point (z_0, t_0) approaches a diffusion transition probability P_f satisfying the diffusion equation, eq. 9, such that

$$P(z, t; z_0, t_0) \rightarrow P_f(z, t; z_0, t_0 + T_{L0}) \quad \text{as } (t - t_0)/T_{L0} \rightarrow \infty \quad (11)$$

where $T_{L0} = T_L(z_0)$. The time delay T_{L0} appears on the right of eq. 11 because it is required to obtain the best far-field match between P and P_f in homogeneous turbulence (see Fig. 2). It follows that P can be decomposed into a far-field, diffusive part, P_f , and a near-field, non-diffusive part, P_n , such that $P_f \rightarrow P$ and $P_n \rightarrow 0$ as $(t - t_0)/T_L \rightarrow \infty$

$$P(z, t; z_0, t_0) = P_f(z, t; z_0, t_0 + T_{L0}) + P_n(z, t; z_0, t_0) \quad (12)$$

The non-diffusive part $P_n = P - P_f$ is large only for $(t - t_0)/T_L \lesssim 1$, a modest range of travel times in which most marked particles do not spread vertically very far from the height, z_0 , of the marking source point and are confined to a height interval with depth of order $\sigma_w(z_0) T_L(z_0)$. Provided the inhomogeneity is not too strong, conditions in this narrow height range will not depart far from homogeneity. This motivates Assumption II: $P_n(z, t; z_0, t_0)$ can be approximated by its value in locally homogeneous turbulence, with velocity and time scales $\sigma_w(z_0)$ and $T_L(z_0)$. Since both P and P_f are known in homogeneous turbulence, P_n is easily found. Assumption II is the reason for the name of the LNF method.

To find the concentration $C(z, t)$, it is also split into a far-field term C_f and a near-field term C_n

$$C(z, t) = C_f(z, t) + C_n(z, t) \quad (13)$$

Putting eq. 12 into eq. 4 (and taking care that the integration of P_f over t_0 does not extend beyond $t_0 + T_{L0} = t$), it follows that

$$C_f(z, t) = \int_0^\infty S(z_0) \int_0^{t - T_{L0}} P_f(z, t; z_0, t_0 + T_{L0}) dt_0 dz_0 \quad (14a)$$

$$C_n(z, t) = \int_0^\infty S(z_0) \int_0^t P_n(z, t; z_0, t_0) dt_0 dz_0 \quad (14b)$$

The diffusive part, C_f , of C can be written down immediately for the non-advective case under consideration (in which t/T_L approaches infinity and $C(z) - C_f(z)$ is independent of t). Since P_f obeys eq. 9, C_f obeys an associated gradient-diffusion relationship of the form of eq. 2

$$F(z) = -K_f(z) dC_f/dz \quad (15)$$

where $K_f(z) = \sigma_w^2(z) T_L(z)$ and where $F(z)$ is related to $S(z)$ by eq. 1. Integrating eq. 15, C_f is found to be

$$C_f(z) = C(z_R) - C_n(z_R) + \int_z^{z_R} \frac{F(z)}{K_f(z)} dz \quad (16)$$

where $C(z_R)$ is a given boundary condition and $C_n(z_R)$ is determined below. This completes the task of writing C_f in terms of S .

Turning now to the non-diffusive part, C_n , it is helpful to introduce the integrated transition probability

$$J(z, t; z_0) = \int_0^t P(z, t; z_0, t_0) dt_0 \quad (17)$$

which is equal to the concentration field at time t from a steady unit point source at z_0 , turned on at $t_0=0$. From eq. 4, $C(z, t)$ can be expressed in terms of J with a single height integral

$$C(z, t) = \int_0^\infty S(z_0) J(z, t; z_0) dz_0 \quad (18)$$

Just as for P and C , J can be decomposed into a diffusive part, J_f , and a non-diffusive part, J_n , such that

$$J(z, t; z_0) = J_f(z, t; z_0) + J_n(z, t; z_0) \quad (19)$$

where J_f and J_n are equal to the inner (time) integrals in eqs. 14a and b, respectively. The relationships between C_f and J_f , and between C_n and J_n , are identical to eq. 18. For the case of homogeneous turbulence, the explicit forms for J and J_f are

$$J(z, t; z_0) = \int_0^t \frac{1}{(2\pi)^{1/2} \sigma_Z(t_1)} \exp \left[-\frac{(z - z_0)^2}{2\sigma_Z^2(t_1)} \right] dt_1 \quad (20a)$$

$$J_f(z, t; z_0) = \int_0^{t-T_{L0}} \frac{1}{(2\pi)^{1/2} \sigma_{Zf}(t_2)} \exp \left[-\frac{(z - z_0)^2}{2\sigma_{Zf}^2(t_2)} \right] dt_2 \quad (20b)$$

where $\sigma_Z(t)$ is defined by eq. 6, and $\sigma_{Zf}(t) = (2\sigma_{w0}^2 T_{L0} t)^{1/2}$ (with $\sigma_{w0} = \sigma_w(z_0)$, $T_{L0} = T_L(z_0)$). The dummy variables t_1 and t_2 are related to t_0 by $t_1 = t - t_0$ and $t_2 = t - T_{L0} - t_0$. Figure 3 shows the time durations of the steady, unit point sources which contribute to the real cloud J and the diffusion cloud J_f , indicating the relationship between the instantaneous real and diffusion releases

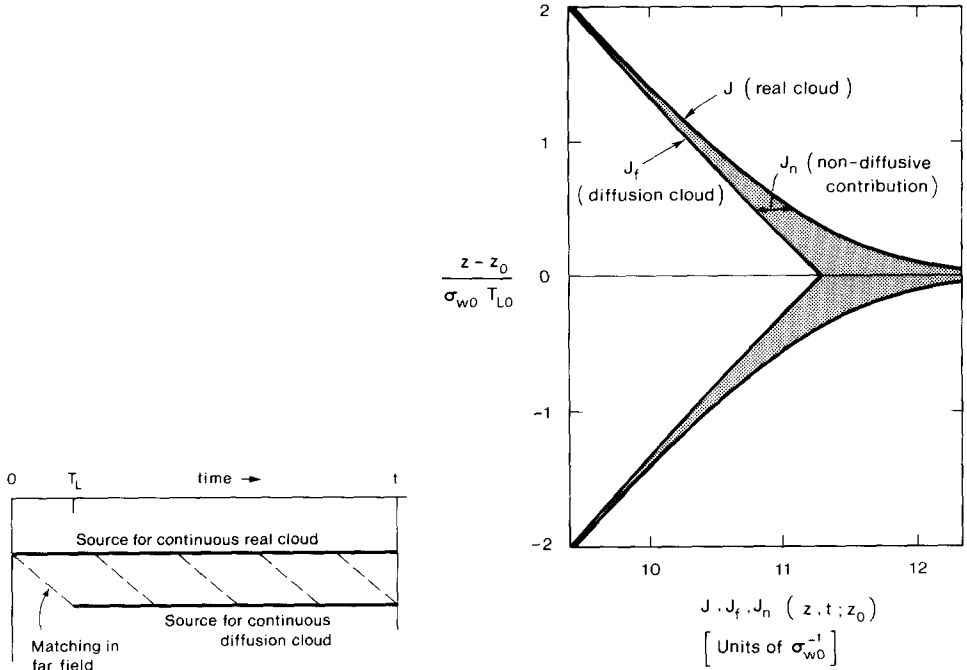


Fig. 3. Relationship between the continuous, point, unit sources, dispersing in the z dimension, which produce the real cloud J and the diffusion cloud J_f .

Fig. 4. $J(z, t; z_0)$ and $J_f(z, t; z_0)$ in homogeneous turbulence. The shaded area represents the difference $J_n(z, t; z_0) = J(z, t; z_0) - J_f(z, t; z_0)$.

which match in the far field, while Fig. 4 shows J , J_f and the difference $J_n = J - J_f$, for homogeneous turbulence.

Assumption II implies that J_n for inhomogeneous turbulence is equal to its value for homogeneous turbulence. This value (the difference between the integrals 20a and 20b) quickly approaches a steady limit as the upper integration limit t increases; in practice, $t/T_{L0} > 5$ is sufficient, because P_n attenuates rapidly with increasing travel time and is negligible for travel times greater than $\sim 5T_{L0}$. In an extensive canopy, the only concern is with J_n at large times, $t \gg 5T_{L0}$, so consideration can be restricted to the steady limit of $J_n(z, t; z_0)$ as $t/T_{L0} \rightarrow \infty$. This limit defines a dimensionless “near-field kernel function”

$$k_n(\zeta) = \lim_{\tau \rightarrow \infty} \sigma_{w0} J_n(\sigma_{w0} T_{L0} \zeta, T_{L0} \tau; 0) \quad (21)$$

where $\zeta = (z - z_0) / (\sigma_{w0} T_{L0})$ and $\tau = t / T_{L0}$ are dimensionless length and time variables, and the factor σ_{w0} is included to non-dimensionalize J_n . The function k_n , shown in Fig. 5, has several useful properties. Firstly, it is symmetric

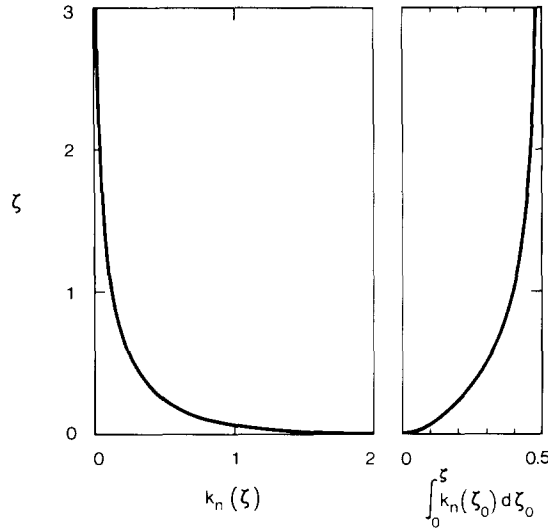


Fig. 5. The near-field kernel function, $k_n(\zeta)$, and its integral with ζ .

in ζ [i.e., $k_n(\zeta) = k_n(-\zeta)$] because J , J_f and J_n are all symmetric in $z - z_0$ for homogeneous turbulence. Secondly, we have

$$\int_{-\infty}^{\infty} k_n(\zeta) d\zeta = 1 \quad (22)$$

[This follows from eq. 20, by which $J(z, t; z_0)$ is the concentration from a steady source with strength (emitted scalar mass per unit time) $F_* = 1$, turned on between 0 and t , and $J_f(z, t; z_0)$ is the concentration of the diffusion cloud from a source with $F_* = 1$, turned on between T_{L0} and t . The J and J_f clouds therefore contain mass $F_* t$ and $F_*(t - T_{L0})$, respectively, so J_n contains mass $F_* T_{L0}$. Non-dimensionalizing with F_* , σ_{w0} and T_{L0} , eq. 22 is obtained.] Thirdly, although no analytic form for $k_n(\zeta)$ is available, a simple and adequate analytic approximation is

$$k_n(\zeta) = -0.39894 \ln(1 - e^{-|\zeta|}) - 0.15623 e^{-|\zeta|} \quad (23)$$

which is derived in Raupach (1989).

From eq. 18 in its form relating C_n to J_n and eq. 21, C_n can be written directly. To apply the homogeneous-turbulence result for k_n to the flow in the canopy, which is bounded at $z = 0$, an image source density and turbulent flow are introduced below the ground, as in the homogeneous-turbulence calculations of Raupach (1987). The result for C_n is

$$C_n(z) = \int_0^\infty \frac{S(z_0)}{\sigma_{w0}} \left[k_n \left[\frac{z-z_0}{\sigma_{w0} T_{L0}} \right] + k_n \left[\frac{z+z_0}{\sigma_{w0} T_{L0}} \right] \right] dz_0 \quad (24)$$

where the zero subscript denotes z_0 dependence: $\sigma_{w0} = \sigma_w(z_0)$, $T_{L0} = T_L(z_0)$. The dependence of C_n on t is dropped because C_n is independent of t for $t \gtrsim 5T_{L0}$, just as for J_n . Equation 24 shows that the near-field contribution $C_n(z)$ is the convolution of S with the near-field kernel function k_n .

The LNF solution to the forward (C from S) problem in non-advective conditions is now complete. We have $C = C_f + C_n$, with C_f given by eq. 16 and C_n by eq. 24. The character of the solution in practice is indicated in Fig. 6, which shows profiles of C and C_f for two source densities, S , typical of daytime heat and water vapour source distributions in forest canopies. The assumed profiles $\sigma_w(z)$ and $T_L(z)$ are also shown. In both $S(z)$ profiles, the upper (crown) peak accounts for 90% of the overall scalar flux density $F_* = F(h)$ from the canopy, while the lower (understorey and ground) peak accounts for the remaining 10%. The upper peak is sharp in Case A, but more vertically diffuse in Case B. Several features are noteworthy: firstly, the main small-scale structure in $C(z)$ is imparted by C_n (the difference between C and C_f), which tends to induce peaks in C at the heights of peaks in S . By comparison, C_f has a much smoother profile which reflects little of the shape of S and serves mainly to set the large-scale variation in C . Secondly, the local peaks in C_n can be strong enough to cause a gradient reversal in $C(z)$ just below a peak in $S(z)$, as in Case A. Because $F(z)$ is positive, this situation represents a countergradient flux. Thirdly, the detailed shape of $C(z)$ is very sensitive to $S(z)$ because of the small-scale structure preserved in C_n . Thus, a minor increase in the spread of the upper

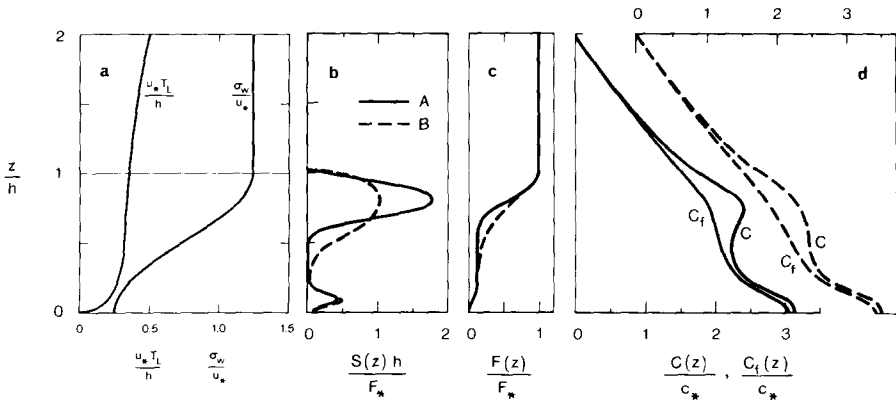


Fig. 6. (a) Assumed profiles of σ_w and T_L ; (b) source density profiles for Cases A and B; (c) flux densities $F(z)$ from eq. 1; (d) far-field and total concentrations $C_f(z)$ and $C(z)$. Normalizing flux and concentration scales are $F_* = F(h)$ and $c_* = F_*/u_*$, respectively.

peak in $S(z)$ causes the countergradient flux observed in Case A to disappear in Case B.

The assumptions of the LNF theory (strictly valid only in weakly inhomogeneous turbulence) have been tested by careful comparisons between LNF and a random-flight model (Sawford, 1986). The results, given in Raupach (1989), show that the LNF assumptions are tenable in turbulence at least as inhomogeneous as that in typical plant canopies. The random-flight model was also used to test the effect of skewness (which is neglected in the LNF theory); it was found that the effect of skewness on the C profile from a given S is trivial for $0 \gtrsim Sk_w \gtrsim -0.5$ and quite small for $Sk_w \gtrsim -1$, ranges which encompass almost all of the data in Fig. 1(c). Hence, the neglect of skewness in the LNF theory appears to be a reasonable simplification.

THE DISPERSION MATRIX AND THE INVERSE PROBLEM

Having obtained a robust, analytic solution to the forward (C from S) problem, practical methods are required for the inverse (S from C) problem. It is convenient to restrict discussion to non-advective conditions, as in the previous section, and to consider the problem in discrete form.

Suppose that the canopy source is divided into m layers, each having a uniform source density, S_j , where $j=1, \dots, m$. The top of layer j is at z_j , with $z_m=h$, and the depth of layer j is $\Delta z_j = z_j - z_{j-1}$. Any flux of scalar from the ground is assumed to be lumped in with the source from the lowest layer (though this is not a necessary simplification). Let us also suppose that there are n heights z_i ($i=1, \dots, n$) at which a profile of mean scalar concentrations C_i ($i=1, \dots, n$) is measured; the top profile height, z_n , coincides with a reference level $z_n = z_R$ above the canopy, at which the concentration is $C_n = C_R$. The source layers ($j=1-m$) and the profile heights for concentration measurement ($i=1-n$) are shown in Fig. 7; it is important that the two sets of heights can be fixed quite independently and need not coincide in any way.

Consider now a scalar tracer which is released uniformly in layer j with source density s ; the tracer source density is zero in all other layers. The resulting tracer concentration profile, c_i , defines a dispersion matrix D with elements D_{ij} is given by

$$D_{ij} = \frac{c_i - c_R}{s \Delta z_j} \quad (25)$$

which is the concentration at measurement height i (relative to the reference concentration at z_R) produced by a uniform unit source, extending vertically throughout layer j , but zero elsewhere. The matrix \mathbf{D} can be calculated from any canopy transfer theory which solves the forward problem and, in particular, can be found from the LNF theory, given the turbulence properties $\sigma_w(z)$ and $T_L(z)$. Once \mathbf{D} is known, the concentration profile from an arbitrary source

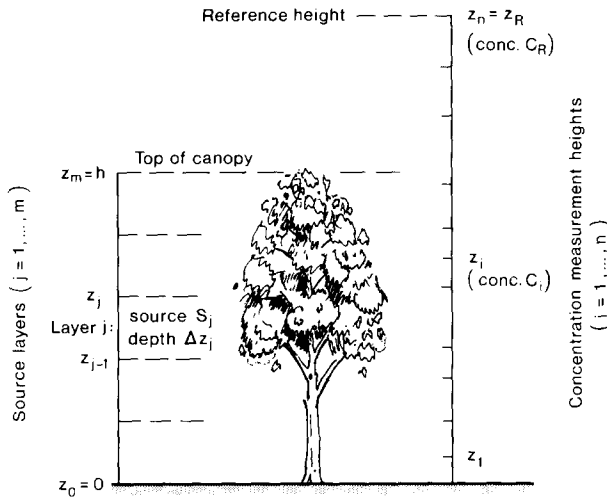


Fig. 7. Source layers and concentration measurement heights for the inverse problem.

profile, S_j , is given by the superposition principle (which states that if source densities S_1 and S_2 produce concentration fields C_1 and C_2 , then $S_1 + S_2$ produces $C_1 + C_2$). It follows that

$$C_i - C_R = \sum_{j=1}^m D_{ij} S_j \Delta z_j \quad (26)$$

This is simply the solution to the forward problem written in discrete form; it is valid whether or not the sources S_j depend on the local ambient concentrations.

The solution to the inverse problem is now straightforward in principle. Choosing $m=n$, so that S_j is sought in the same number of source layers as there are concentration values C_i , eq. 26 becomes a set of m linear equations which can be solved for the source profile S_j . Hence, the solution is unique (since linearity ensures uniqueness) and it is also mathematically easy. However, it is not necessarily stable: small errors in C_i , $\sigma_w(z)$ or $T_L(z)$ may well be amplified to produce unacceptable errors in the inferred S_j . Preliminary attempts at solving eq. 26 for S_j , using measured concentration profile data at $n=m$ heights, showed clearly that the instability is catastrophic.

The way to overcome this problem is to include redundant concentration data, so that source densities, S_j , in m layers are sought from n measured concentration values, \hat{C}_i , with $n > m$. The S_j values producing the best fit to the measured \hat{C}_i can be found with a least squares procedure, by minimizing the squared error (ϵ) defined by

$$\epsilon = \sum_{i=1}^n (C_i - \hat{C}_i)^2 \quad (27)$$

where C_i are the predicted concentrations from eq. 26. Substituting these into eq. 27, ϵ becomes

$$\epsilon = \sum_{i=1}^n \left[\sum_{j=1}^m D_{ij} S_j \Delta z_j - (\hat{C}_i - C_R) \right]^2 \quad (28)$$

The S_j values which minimize ϵ are given by

$$\partial \epsilon / \partial S_j = 0 \quad (j=1, \dots, m) \quad (29)$$

which is a set of m linear equations in the unknowns, S_j , taking the explicit form

$$\sum_{k=1}^m A_{jk} S_k = B_j \quad (j=1, \dots, m) \quad (30)$$

where the matrix with elements A_{jk} and the vector with elements B_j are defined by

$$A_{jk} = \sum_{i=1}^n D_{ij} \Delta z_j D_{ik} \Delta z_k \quad (31a)$$

$$B_j = \sum_{i=1}^n (\hat{C}_i - C_R) D_{ij} \Delta z_j \quad (31b)$$

Hence, eq. 30 replaces eq. 26 as a set of equations for m values of S_j . The inherent redundancy (when $n > m$) ensures that the resulting solution, S_j , is not oversensitive to \hat{C}_i . When there is no redundancy ($n = m$), eq. 30 degenerates to the original equation set, eq. 26.

HOW MUCH TURBULENCE INFORMATION IS REQUIRED?

Like the forward (C from S) problem in a Lagrangian framework, the inverse (S from C) problem can only be solved when certain turbulence statistics are specified in advance. The solution developed here requires profiles of $\sigma_w(z)$ and $T_L(z)$, which determine the dispersion matrix \mathbf{D} . Normally, one will not have the luxury of a complete set of turbulence measurements to determine these profiles; and even if extensive turbulence data are available, there remains the problem of inferring T_L from Eulerian turbulence data, as discussed briefly above. Hence, it is usually necessary to estimate profiles of σ_w and T_L , using scaling laws and simple, assumed profile shapes within the canopy which are consistent with existing data such as Fig. 1. For example, Raupach (1988) suggested that $\sigma_w(z)$ and $T_L(z)$ may be approximated by the piecewise linear profiles shown in Fig. 8, which obey

$$\sigma_w(z)/u_* = a_1 \quad (z/h > 1) \quad (32a)$$

$$\sigma_w(z)/u_* = a_0 + (a_1 - a_0)z/h \quad (z/h \leq 1) \quad (32b)$$

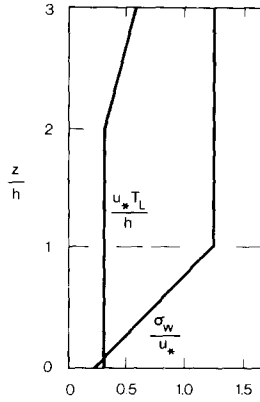


Fig. 8. Assumed simple profile shapes for σ_w and T_L .

$$\frac{T_L(z)u_*}{h} = \max \left[c_0, \frac{k(z-d)}{a_1 h} \right] \quad (33)$$

where k is the von Karman constant and d the zero-plane displacement, so that the term proportional to $(z-d)$ in eq. 33 is the inertial sub-layer form for T_L which applies well above the canopy. For approximate consistency with most of the data in Fig. 1, the constants are $a_1 = 1.25$, $a_0 = 0.25$, $c_0 = 0.3$.

Clearly, $\sigma_w(z)$ and $T_L(z)$ in any specific canopy will only approximately conform to such an idealization. It is therefore necessary to investigate the extent to which an inferred source profile, S_j , is sensitive to erroneous assumptions about $\sigma_w(z)$ and $T_L(z)$. To do this, eq. 26 was used to calculate the concentration profile, C_i , for a given, initial source profile, with \mathbf{D} determined by using $\sigma_w(z)$ and $T_L(z)$ from eqs. 32 and 33 as “correct” turbulence profiles. The calculated C_i was then used to predict the source profile S_j by solving eq. 30, using a \mathbf{D} determined from altered, “incorrect” profiles of σ_w and T_L . The difference between the initial and final source profiles indicates the sensitivity of eq. 30 to σ_w and T_L .

Figure 9 shows an example of such a calculation in which $\sigma_w(z)$ is perturbed while holding $T_L(z)$ equal to its initial, “correct” form. The initial source profile was bimodal, similar to Source B in Fig. 6. This initial $S(z)$ and the corresponding flux profile $F(z)$ (obtained from eq. 1 with $F_g = 0$) are shown as heavy solid lines in Fig. 9(b) and (c), respectively. Figure 9(a) shows four “incorrect” assumptions about $\sigma_w(z)$, each a linear profile; they were obtained by increasing and decreasing σ_w near the top of the canopy and likewise near the bottom of the canopy. The inferred $S(z)$ and $F(z)$ profiles obtained with these “incorrect” σ_w profiles are shown in Fig. 9(b) and (c). In general terms, a fairly straightforward result is obtained: where σ_w is erroneously high, an

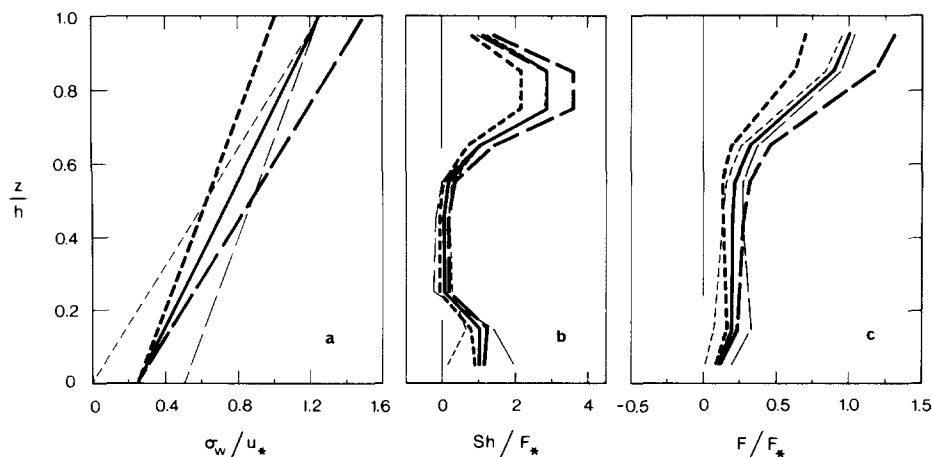


Fig. 9. Sensitivity of the solution to the inverse problem with respect to σ_w , with T_L held constant as in Fig. 8. (a) Perturbed σ_w profiles; (b) inferred perturbed S profiles; (c) inferred perturbed F profiles. Heavy solid lines in (b) and (c) indicate original, unperturbed profiles of S and F .

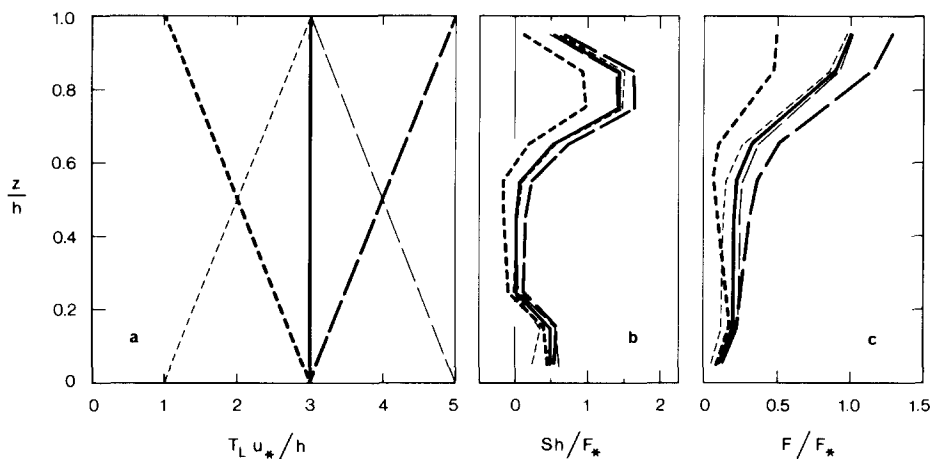


Fig. 10. Sensitivity of the solution to the inverse problem with respect to T_L , with σ_w held constant as in Fig. 8. (a) Perturbed T_L profiles; (b) inferred perturbed S profiles; (c) inferred perturbed F profiles. Heavy solid lines in (b) and (c) indicate original, unperturbed profiles of S and F .

erroneously high $S(z)$ value is inferred, and vice versa. A given fractional error in σ_w induces a somewhat higher fractional error in $S(z)$.

Figure 10 shows the results of a similar calculation in which $T_L(z)$ is perturbed while $\sigma_w(z)$ is held constant at its "correct" form. A very similar overall result is obtained: a high T_L leads to an overestimate of $S(z)$ and vice versa. A given fractional error in T_L induces a lower fractional error in $S(z)$, in contrast to the case of σ_w , so T_L is a less sensitive parameter in the calculation than σ_w .

This is useful because σ_w can be directly measured, in principle, with sonic anemometers or other turbulence sensors, whereas T_L is hard to infer from Eulerian measurements, as already discussed. The calculations leading to Figs. 9 and 10 have been repeated for various other initial source profiles, always with the same general conclusions.

EXAMPLE OF CALCULATION OF S FROM C

The solution to the inverse problem has been tested with turbulence and concentration data from a wind tunnel experiment on scalar dispersion from an elevated plane source within a canopy (Coppin et al., 1986). The experiment was carried out in the WT Strips canopy (Fig. 1 and Table 1). The passive scalar was heat, released at a power $H_s = 275 \text{ W m}^{-2}$ from an array of wires stretched laterally between the elements, at a height of $0.8h$ ($h = 60 \text{ mm}$). The turbulence profiles used to calculate \mathbf{D} are shown in Fig. 11(a); the σ_w profile closely resembles the data in Fig. 1(a), while the T_L profile follows the profile of L_w/σ_w in Fig. 1(b) with somewhat more abstraction. A particular measured temperature (scalar concentration) profile was chosen randomly from the data set (see Fig. 11(b)). This was done in preference to using an averaged temperature profile to see the effect of noise in the data. Figure 11(c) and (d) shows the heat source density profile, $S_H(z)$, and the heat flux profile, $H(z)$, inferred from that temperature profile using eq. 30. The calculations were done for both $m=4$ and $m=8$ source layers in the canopy (solid and dashed lines, respectively).

The predictions of H from eq. 30 may be compared with the measured eddy covariance heat flux profile and also with the value H_s of the electrically ap-

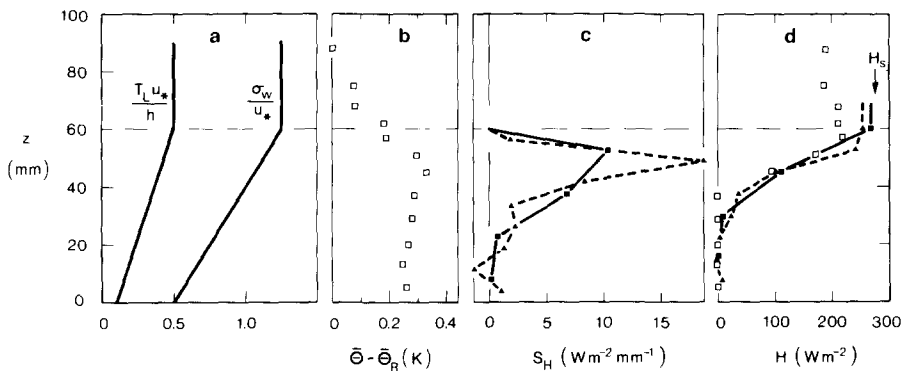


Fig. 11. Test of the solution to the inverse problem with data from an experiment on the dispersion of trace heat from an elevated plane source in a wind tunnel model canopy. (a) Assumed σ_w and T_L profiles; (b) measured temperature profile; (c) inferred profile of heat source density S_H ; (d) inferred heat flux profile. Solid lines, $m=4$; dashed lines, $m=8$; squares in (d), measured eddy covariance heat flux; arrow in (d), applied electrical power.

plied heat flux (both shown in Fig. 11(d)). The eddy covariance heat flux at canopy height h is $\sim 20\%$ less than H_s because of some advection in the canopy (accounting for $\sim 10\%$) and also some high-frequency and high-wave-number loss in the eddy covariance measurements (accounting for the other 10%). Bearing this in mind, there is good agreement between the measured heat flux profile and those inferred from eq. 30. The noise in the temperature profile does not appear as an unacceptable noise level in the inferred S_H profile, although naturally the S_H profile with $m=8$ is noisier than that with $m=4$.

A final point concerns the choice of T_L . The T_L profile in Fig. 11(a) is based on the L_w/σ_w profile in Fig. 1(b), with the assumption that $\beta=1$ in eq. 3. In other words, this T_L profile is inferred from single-point turbulence data. It is somewhat different from the diffusivity-based T_L profile deduced by Legg et al. (1986) using the measured far-field diffusivity from a lateral line source in the same canopy, also at height $0.8h$; that T_L profile suggests $T_L u_* / h \sim 0.3$ in the canopy, with little height variation. It is quite possible that the disagreement between the two T_L profiles is due simply to measurement error, since the diffusivity-based T_L values were inferred from very small far-field fluxes and gradients which tested the resolution of the instrumentation. If the diffusivity-based T_L profile is used instead of the one based on single-point turbulence data, then the agreement between measured and inferred flux profiles is substantially worsened; the inferred H value at $z=h$ reduces from ~ 260 to 160 W m^{-2} in comparison with $H_s = 275 \text{ W m}^{-2}$. This provides some indication that T_L values inferred from single-point turbulence data, using eq. 3 with $\beta=1$, may be reasonable.

CONCLUSIONS

I have distinguished two problems which a theory of scalar transfer in canopies must address: the “forward problem” of predicting the mean concentration profile $C(z)$ from a given source density profile $S(z)$, and the “inverse problem” of predicting $S(z)$ from a given $C(z)$. An analytic Lagrangian dispersion theory, labelled LNF theory, offers a practical solution to the forward problem. The theory is based on two assumptions: (I) that dispersion in the far field is diffusive, satisfying the diffusion equation and hence a gradient-diffusion relationship with the far-field eddy diffusivity $K_f(z) = \sigma_w^2(z) T_L(z)$, where σ_w and T_L are the standard deviation and Lagrangian time scale for vertical velocity; and (II) that near-field effects close to a particular source point in the canopy can be treated by regarding the turbulence as homogeneous with values of σ_w and T_L equal to those at the source point. Both assumptions are exact in the homogeneous-turbulence limit, but adequate in the inhomogeneous turbulence typically found in canopies. The theory leads to a simple expression for $C(z)$ in terms of $S(z)$, which is obtained by expressing $C(z)$ as the sum of a diffusive, far-field contribution $C_f(z)$ and a non-diffusive, near-

field contribution $C_n(z)$: $C(z) = C_f(z) + C_n(z)$. Expressions for C_f and C_n are given in eqs. 16 and 24.

The LNF theory for the forward (C from S) problem yields the conclusion that $C(z)$ carries substantial information about $S(z)$ through the near-field contribution, $C_n(z)$, which is the convolution of S with a “near-field kernel function” k_n (see eq. 23 and Fig. 5). In other words, peaks in $S(z)$ produce peaks in $C_n(z)$ and thence tend to produce peaks in $C(z)$ (see Fig. 6 and the associated discussion). This explains observations of countergradient fluxes, since peaks in $C(z)$ imply gradient reversal without flux reversal. More importantly, though, the possibility is raised of inferring S from measurements of C ; that is, of solving the inverse (S from C) problem. Because k_n is a very sharply peaked function of height, $C_n(z)$ contains a detailed “signature” of $S(z)$ with little smoothing in z , so in principle it should be possible to infer $S(z)$ with high resolution in z . In this respect, the inverse problem in a canopy is akin to deconvolution problems in astrophysical image resolution.

The practical approach to the inverse problem is to define a “dispersion matrix”, \mathbf{D} , such that an element D_{ij} is equal to the concentration at measurement height i (relative to a reference concentration above the canopy) produced by a uniform unit source in layer j of the canopy. The dispersion matrix can be found with the LNF theory for the forward problem (though another theory could also be used). According to the LNF theory, \mathbf{D} is a property of the turbulence statistics $\sigma_w(z)$ and $T_L(z)$, which must be known by measurement or assumed from scaling laws. The superposition principle implies that a concentration profile C_i and a source density profile S_j (both in discrete form) are related linearly by \mathbf{D} , so the inverse problem is reduced to the solution of a set of linear equations with unknowns S_j and coefficients D_{ij} . In practice, it is necessary to use a least-squares method to fit values of S_j in m canopy layers to a measured n -point concentration profile where $n > m$, so that there is enough redundant information in the concentration profile to make the solution, S_j , stable to noise in the concentration profile.

The practicality of the solution to the inverse problem has been tested in two ways. Firstly, sensitivity tests show that the solution to the inverse problem is not unduly sensitive to either σ_w or T_L , though the sensitivity is higher for σ_w than T_L . Secondly, the solution has been tested with wind-tunnel data on the dispersion of trace heat from an elevated plane source in a canopy. Good agreement was found between the directly measured heat flux profile from eddy covariance and the heat flux profile inferred by applying the solution of the inverse problem to a measured temperature profile.

For field application of the solution to the inverse problem, σ_w and T_L would normally be inferred from one (or at most a few) sonic anemometers, using L_w/σ_w as an approximation for T_L (where L_w is the single-point Eulerian length scale for vertical velocity). It remains to be seen whether this level of turbu-

lence information is adequate for inferring $S(z)$ from measurements of $C(z)$ in field canopies.

ACKNOWLEDGEMENTS

I am grateful to Drs. D.E. Aylor, J.J. Finnigan and J.B. Passioura for discussions and comments on a draft of this paper, and especially to Dr. O.T. Denmead for posing the inverse problem in the form addressed here.

REFERENCES

- Batchelor, G.K., 1949. Diffusion in a field of homogeneous turbulence. I. Eulerian analysis. *Aust. J. Sci. Res.*, 2: 437-450.
- Coppin, P.A., Raupach, M.R. and Legg, B.J., 1986. Experiments on scalar dispersion within a plant canopy, part II: An elevated plane source. *Boundary-Layer Meteorol.*, 35: 167-191.
- Corrsin, S., 1963. Estimates of the relations between Eulerian and Lagrangian scales in large Reynolds number turbulence. *J. Atmos. Sci.*, 20: 115-119.
- Corrsin, S., 1974. Limitations of gradient transport models in random walks and in turbulence. *Adv. Geophys.*, 18A: 25-60.
- Denmead, O.T. and Bradley, E.F., 1985. Flux-gradient relationships in a forest canopy. In: B.A. Hutchison and B.B. Hicks (Editors), *The Forest-Atmosphere Interaction*. Reidel, Dordrecht, pp. 421-442.
- Denmead, O.T. and Bradley, E.F., 1987. On scalar transport in plant canopies. *Irrig. Sci.*, 8: 131-149.
- Durbin, P.A., 1983. Stochastic differential equations and turbulent dispersion. NASA Ref. Publ. 1103.
- Finnigan, J.J. and Raupach, M.R., 1987. Transfer processes in plant canopies in relation to stomatal characteristics. In: E. Zeiger, G.D. Farquhar and I.R. Cowan (Editors), *Stomatal Function*. Stanford University Press, Stanford, CA, pp. 385-429.
- Legg, B.J., Raupach, M.R. and Coppin, P.A., 1986. Experiments on scalar dispersion within a plant canopy, part III: an elevated line source. *Boundary-Layer Meteorol.*, 35: 277-302.
- Monin, A.S. and Yaglom, A.M., 1971. *Statistical Fluid Mechanics: Mechanics of Turbulence*, Vol. 1. M.I.T. Press, Cambridge, MA, U.S.A. [English Translation; J.L. Lumley (Editor)] 769 pp.
- Raupach, M.R., 1987. A Lagrangian analysis of scalar transfer in vegetation canopies. *Q. J. R. Meteorol. Soc.*, 113: 107-120.
- Raupach, M.R., 1988. Canopy transport processes. In: W.L. Steffen and O.T. Denmead (Editors), *Flow and Transport in the Natural Environment: Advances and Applications*. Springer-Verlag, Berlin, pp. 95-127.
- Raupach, M.R., 1989. A practical Lagrangian method for relating scalar concentrations to source distributions in vegetation canopies. *Q. J. R. Meteorol. Soc.*, in press.
- Raupach, M.R., Coppin, P.A. and Legg, B.J., 1986. Experiments on scalar dispersion within a plant canopy, part I: The turbulence structure. *Boundary-Layer Meteorol.*, 35: 21-52.
- Sawford, B.L., 1984. Lagrangian statistical modelling of turbulent dispersion. *Proceedings of the 8th International Clean Air Conference*, pp. 17-27.
- Sawford, B.L., 1986. Generalized random forcing in random-walk turbulent dispersion models. *Phys. Fluids*, 29: 3582-3585.
- Seginer, I., Mulhearn, P.J., Bradley, E.F. and Finnigan, J.J., 1976. Turbulent flow in a model plant canopy. *Boundary-Layer Meteorol.*, 10: 423-453.

- Shaw, R.H., Silversides, R.H. and Thurtell, G.W., 1974. Some observations of turbulence and turbulent transport within and above plant canopies. *Boundary-Layer Meteorol.*, 5: 429-449.
- Snyder, W.H. and Lumley, J.L., 1971. Some measurements of particle velocity autocorrelation functions in a turbulent flow. *J. Fluid Mech.*, 48: 41-71.
- Taylor, G.I., 1921. Diffusion by continuous movements. *Proc. London Math. Soc.*, A20: 196-211.
- Tennekes, H. and Lumley, J.L., 1972. *A first course in turbulence*. M.I.T. Press, Cambridge, MA, 300 pp.
- Thomson, D.J., 1987. Criteria for the selection of stochastic models of particle trajectories in turbulent flows. *J. Fluid Mech.*, 180: 529-556.
- Wilson, J.D., Ward, D.P., Thurtell, G.W. and Kidd, G.E., 1982. Statistics of atmospheric turbulence within and above a corn canopy. *Boundary-Layer Meteorol.*, 24: 495-519.